Plant Science 175 (2008) 717–723

Contents lists available at ScienceDirect

Plant Science

journal homepage: www.elsevier.com/locate/plantsci

Proteome analysis of secondary somatic embryogenesis in cassava (*Manihot esculenta*)

Abdulrazak I. Baba [a], Fabio C.S. Nogueira [b], Camila B. Pinheiro [b], Juliana N. Brasil [b], Emmanuel S. Jereissati [b], Thiago L. Jucá [b], Arlete A. Soares [d], Marise F. Santos [c], Gilberto B. Domont [c], Francisco A.P. Campos [b,*]

[a] *Department of Biochemistry, Ahmadu Bello University, Zaria, Nigeria*
[b] *Department of Biochemistry and Molecular Biology, Federal University of Ceará, PO Box 6039, Fortaleza 60455-900, Ceará, Brazil*
[c] *Chemistry Institute, Federal University of Rio de Janeiro, Rio de Janeiro, Brazil*
[d] *Department of Biology, Federal University of Ceará, Fortaleza, Ceará, Brazil*

ARTICLE INFO

Article history:
Received 19 March 2008
Received in revised form 8 July 2008
Accepted 24 July 2008
Available online 9 August 2008

Keywords:
Manihot esculenta
Proteome analysis
Mass spectrometry
Somatic embryogenesis
Secondary somatic embryogenesis

ABSTRACT

Using histological analysis of the induction of secondary somatic embryogenesis (SSE) in cassava (*Manihot esculenta* Crantz) as a guide, we performed 2-DE for protein separation and matrix-assisted laser desorption ionization-time of flight-tandem mass spectrometry (MALDI-TOF-TOF-MS) for protein identification in cotyledons of cassava somatic embryos undergoing SSE. Reference map obtained by 2-DE within a pH range of 3–10 and a size range of 6–97 kDa revealed approximately 410 eletrophoretically resolved spots populated primarily by acidic ($pI < 7$) proteins with molecular masses between 30 and 75 kDa. Tryptic digestion of 163 of the most abundant spots led to the identification of 86 proteins with a protein identification success rate of 53%. In total, 43% of the identified proteins were involved in metabolism and energy and 11.6% in protein destination and storage. Others are, disease/defense (11.6%), transcription and protein synthesis (7%), signal transduction (5.8%), cell growth/division (3.5%), transporters (3.5%), cell structure (2.3%), secondary metabolism (1.2%) and other functional classes (10.5%). Our studies demonstrate that 2-DE-based proteomic approaches combined with histological studies can serve as tools for identifying protein markers for the developmental stages of cassava SE while providing clues on the underlying causes of the low rate of conversion of cassava somatic embryos into mature plants.

1. Introduction

Cassava (*Manihot esculenta* Crantz) is an important root crop that is the source of staple starch food for more than 700 million people, particularly in the developing countries of Africa, Asia and South America [1]. The new technologies for plant regeneration and transformation are opening up new possibilities to generate improved cassava genotypes by integrating desired traits into farmer-preferred cultivars [2]. Most of the protocols for producing transgenic cassava rely on the use of embryogenic tissues as targets for gene transformation [3–6]. In cassava, somatic embryogenesis (SE) is easily achieved by incubating explants such as young leaves or isolated shoot apexes in culture medium supplemented with auxins such as picloram [7]. Green cotyledons of somatic embryos, when incubated in culture medium supplemented with auxin, produce large numbers of somatic embryos through secondary somatic embryogenesis (SSE) [7,8]. However, the recovery of complete plants from cassava somatic embryos is a challenging task, especially due to the low frequency of embryo germination and this caveat has prevented the generation of transgenic cassava from a wider range of genotypes.

Recent genomic tools, advanced DNA sequencing programs, and expressed sequence tag (EST) libraries have been developed for cassava [9], and researchers have taken advantage of these resources to initiate proteome reference maps for cassava roots using a combination of two-dimensional gel electrophoresis (2-DE) and matrix-assisted laser desorption ionization time-of-flight mass spectrometry (MALDI-TOF-MS) [10]. 2-DE-based proteomic approaches have been applied to investigate molecular changes

* Corresponding author. Tel.: +55 85 33669824; fax: +55 85 33669829.
E-mail address: bioplant@ufc.br (Francisco A.P. Campos).

Abbreviations: SSE, Secondary somatic embryogenesis; SE, Somatic embryogenesis; 2,4-D, 2,4-dichlorophenoxyacetic acid; 2-DE, Two-dimensional electrophoresis; MALDI-TOF-TOF-MS, Matrix-assisted laser desorption ionization-time of flight-tandem mass spectrometry; EST, Expressed sequence tag.

0168-9452/$ – see front matter © 2008 Elsevier Ireland Ltd. All rights reserved.
doi:10.1016/j.plantsci.2008.07.014

during SE in several species [11–16] and it can be expected that the analysis of gene expression during SSE in cassava can provide information about somatic embryo development and thereby providing clues on the underlying causes of the low rate of conversion of cassava somatic embryos into mature plants. In this study we have performed a histological analysis of the induction of SSE in cassava and applied 2-DE for protein separation and MALDI-TOF-TOF-MS for protein identification in cotyledons of cassava somatic embryos undergoing SSE. We have identified 85 protein spots and classified the functions of the proteins related to these spots. The results obtained demonstrate that proteomics can be used for large-scale identification of proteins in mature and developing cassava somatic embryos.

2. Methods

2.1. Chemicals

All chemicals used were of the highest available grade and are described in Vasconcelos et al. [17] unless otherwise indicated. Milli-Q quality water (Millipore, Bedford, MA, USA) was used throughout.

2.2. Plant materials, tissue culture and microscopic analysis

In vitro cultures of the cassava cultivar Rosinha were established from stem cuttings of 20–30 cm obtained from mature plants, as described by Feitosa et al. [7]. For the induction of SE, the explants used were shoot apexes containing up to three leaf primordia isolated from *in vitro* grown plants. The apexes were transferred to Petri dishes containing 25 ml of solidified Murashige and Skoog (MS) medium [18] supplemented with 2% sucrose, 0.5 mg/L copper sulphate and picloram at 12 mg/L and solidified with 0.6% agar. After 3 weeks of incubation under dark conditions at 26 ± 2 °C, clusters consisting of approximately 10 somatic embryos were transferred to maturation medium, which consisted of MS salts and vitamins supplemented with 0.5 mg/L copper sulphate and benzyl adenine (BA) at 0.1 mg/L and solidified with 0.6% agar, and incubated for 3–4 weeks at 26 ± 2 °C under a 16 h photoperiod. Green cotyledons from 2- to 3-week-old mature somatic embryos were used as source of explants for inducing secondary (cyclic) somatic embryogenesis. Cut pieces of green cotyledons each about 5 mm^2 were obtained and transferred to Petri dishes containing 25 mL of solidified MS medium supplemented with 2% sucrose, 0.5 mg/L copper sulphate and picloram at 12 mg/L and solidified with 0.6% agar with the abaxial side of the cotyledon pieces in direct contact with the medium. After 3 weeks of incubation under dark conditions at 26 ± 2 °C, the cultures were scored for the presence of somatic embryos. For histological studies, 5 mm^2 of cut pieces of green cotyledons of somatic embryos were incubated for 1, 3, 6, 12, 16 and 21 days in maturation medium, harvested and fixed in Karnovsky solution for 24 h at room temperature. This was followed by dehydration in an ethanol, *n*-propanol, and *n*-butanol series. The tissues were then embedded in historesin (Leica Microsystems Nussloch GmbH, Germany) following the standard procedures. Serial sections cut at 5–7 μm thickness on a rotary microtome equipped with a steel knife were stained in 0.05% toluidine blue and mounted. Slides were examined under bright field optics in a Zeiss Photomicroscope III.

2.3. Protein extraction, 2-DE separation, in gel trypsin digestion, mass spectrometry analysis, database search and protein identifications

Protein extraction from explants undergoing SSE, as well as 2-DE and image analysis were performed essentially as described by Vasconcelos et al. [17]. Protein spots were excised from Coomassie-stained polyacrylamide gels, destained and digested with sequencing-grade modified trypsin (Promega, Madison, WI, USA). MALDI-TOF-TOF-MS acquisition was performed by an ABI

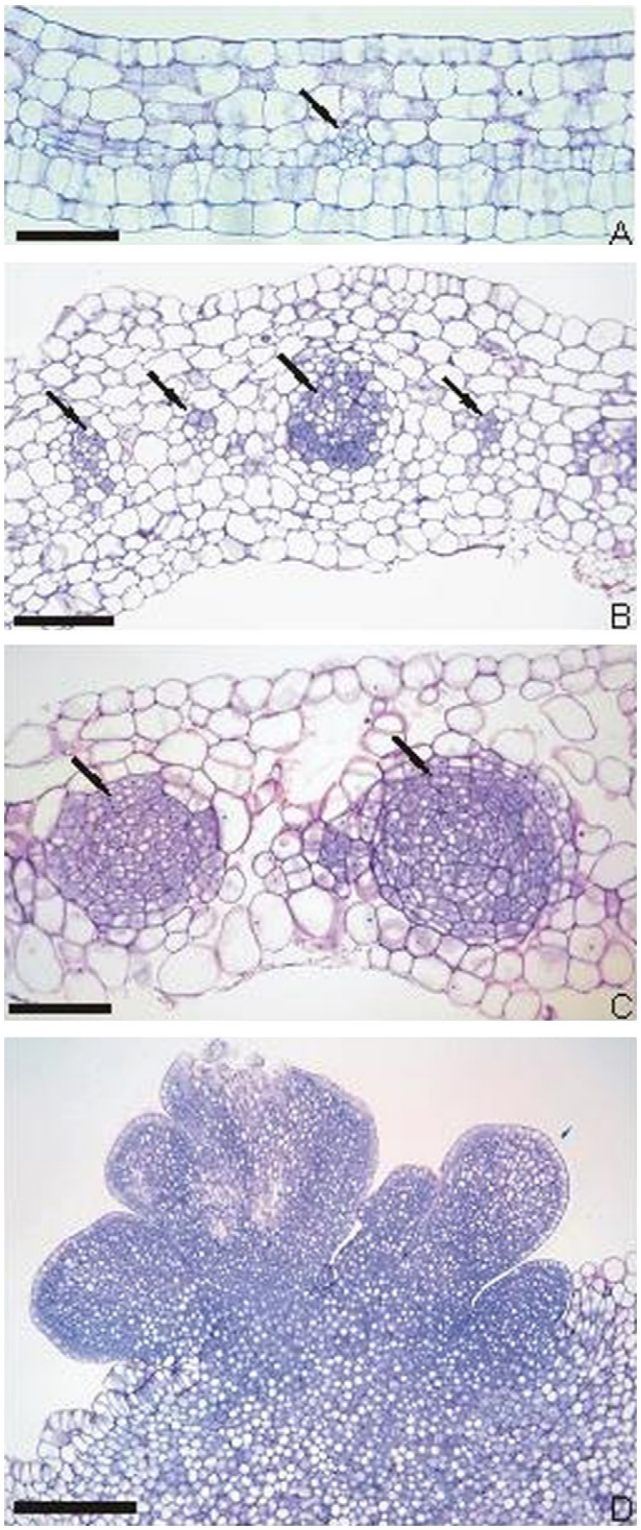

Fig. 1. Histological analysis of the induction of secondary somatic embryogenesis in cassava. Green cotyledons of somatic embryos (A) were incubated in induction medium for 3 (B), 6 (C) and 16 (D) days. Observe the intense cell mitotic activities (arrows) in the vicinities of the vascular bundles. Bars: 100 μm (A–C), and 200 μm (D). (For interpretation of the references to color in this figure legend, the reader is referred to the web version of the article.)

4700 Proteomics Analyzer (Applied Biosystems) using 3,5-dimethoxy-4-hydroxycinnamic acid as matrix and the data obtained were analyzed using the software GPS Explorer™ (Applied Biosystems). The acquired mass spectral data were queried against the NCBI database using the MASCOT (version 1.8.0, Matrix Science, Ltd., London, UK) search engine. Searches were conducted using a mass accuracy of ±100 ppm. Cysteine residues were reduced and alkylated by iodoacetamide to carboxyamidomethyl cysteine and methionine residues modified to methionine sulfoxide wherever necessary. A homology search was performed against the NCBI protein databases. "Viridiplantae taxa" was chosen initially from the taxonomy category.

3. Results and discussion

Within 3 days of incubation of green cotyledons of cassava somatic embryos in induction medium, several histological and anatomical changes in the explants could be observed (Fig. 1), such as an increase in the number of cell layers, in the size of the parenchyma cells and in the number of chloroplasts. Cell divisions at the procambium region gave rise to cells with a dense cytoplasm (Fig. 1B). After 6 days of incubation, there was a dramatic increase in the size of the procambium region, in which meristematic cells of small size, dense cytoplasm, and with prominent nuclei were undergoing intense cell division (Fig. 1C). Increase in the intracellular space outside the procambium region could be observed at this stage. It was also possible to observe, in some explants, the breakdown of the protoderm and the fusion of the cell masses originating from the procambium, such that two types of tissues could be distinguished in the explants: a peripheral one composed of big, highly vacuolated cell and an internal one composed of pre-embryogenic masses. Sixteen days after incubation, somatic embryos at distinct developmental stages could be observed in all explants (Fig. 1D), indicating that in cassava, as in other species such as soybean [19], *Stylosanthes scabra* [20], *Carya illinoiensis* [21] and *Vitis* spp., somatic embryogenesis is not synchronous. Upon transfer to culture medium supplemented with benzyl adenine, the embryo clusters will give rise to mature embryos [7].

The description of the morphology of early SSE in cassava presented here, have permitted us to establish a morphological timetable which allows for accurate selection of induction stages of secondary somatic embryogenesis at relatively narrow intervals over the entire induction period. This also offered the opportunity for material to be reproducibly selected for obtaining proteome reference maps of the various induction and developmental stages. As an initial step in this direction, we set out to identify proteins present in green cotyledons of cassava somatic embryos undergoing SSE for 16 days (Fig. 1D), through the use of two-dimensional electrophoresis (2-DE) and mass spectrometry techniques. The proteome of SSE was profiled using 2-DE within a pH range of 3–10 and a size range of 6–97 kDa and detected by Coomassie brilliant blue staining. Multiple 2-DE gels were acquired, and the best gel was selected to serve as the reference map (Fig. 2). Analytical and biological variances were calculated for triplicate 2-DE gels obtained for similar but independent samples. The reference map contained approximately 410 eletrophoretically resolved protein spots and was populated primarily by acidic ($pI < 7$) proteins but also contained a limited number of basic proteins. The vast majority of proteins visualized possessed molecular masses between 30 and 75 kDa. A total of 163 of the most abundant spots were excised, digested in-gel with trypsin and analyzed by tandem

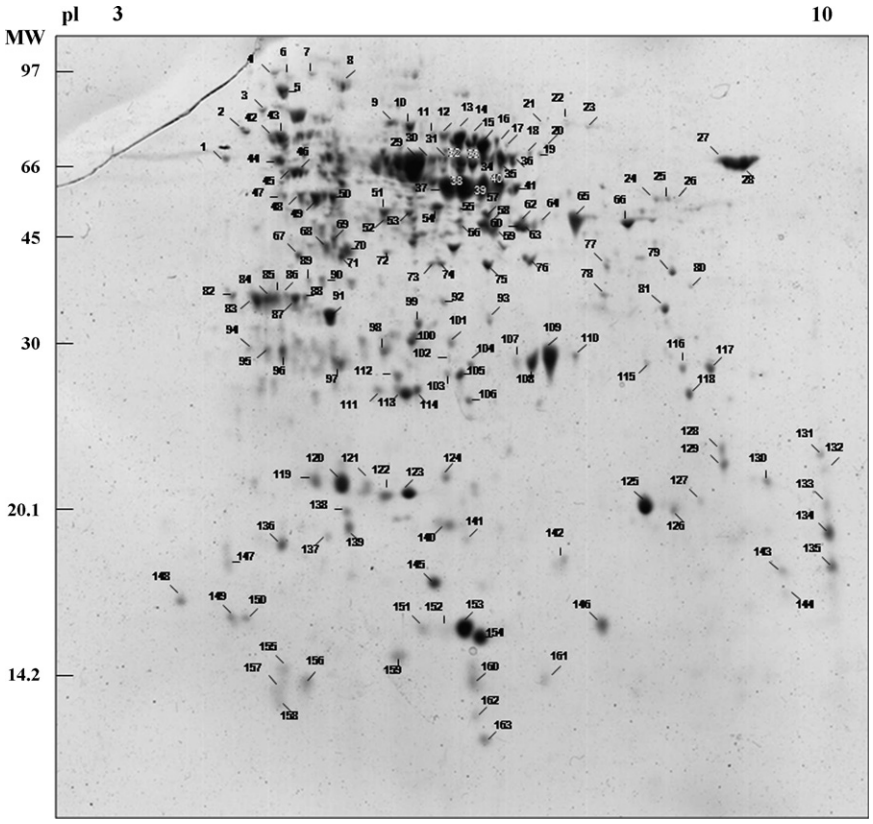

Fig. 2. Analysis of proteins isolated from green cotyledons of cassava somatic embryos undergoing secondary somatic embryogenesis, by 2-DE in combination with colloidal Coomassie Brilliant Blue staining. Protein load was 600 μg and the separation in the first dimension was carried out in IPG strips in the pH range of 3–10. Protein spots were assigned arbitrary identifiers as shown in Table 1.

Table 1
List proteins identified in green cotyledons of cassava somatic embryos undergoing SSE by MALDI-TOF-TOF mass spectrometry

Spot n.[a]	MW (kDa)/p*I*		Prot. score/ion score[c]	Seq. ID Peptides[d]	ID (NCBI)[e]	Protein description
	Exp.[b]	Theor.[b]				
Metabolism and energy						
8	82.2/5.2	92.3/5.4	148/86	DDNPIGATLIGR YDSPFHSLFR AYVPVEELLDGEEIDR LEGPIAWDVLFNFEQR	gi|1698844	Phospholipase D
20	66.9/7.2	30.9/8.7	97/56	DITLGFVDLLR TFQGPPHGIQVER	gi|33669443	Ribulose-1,5-bisphosphate carboxylase/oxygenase large subunit
29	64.5/5.8	50.0/6.8	329/249	DTDILAAFR DITLGFVDLLR TFQGPPHGIQVER	gi|5833911	Ribulose 1,5-bisphosphate carboxylase large subunit
30	63.8/6.0	52.2/5.9	168/123	DITLGFVDLLR TFQGPPHGIQVER	gi|703201	Ribulose 1,5-bisphosphate carboxylase large subunit
151	12.7/5.9	20.6/8.3	204/110	IIGFDNVR AHGSLPGYYDGR EQLASEIDYLLR	gi|6272551	Ribulose 1,5-bisphosphate carboxylase small chain precursor
152	12.8/6.2	20.6/8.3	173/62	AHGSLPGYYDGR EQLASEIDYLLR	gi|6272551	Ribulose 1,5-bisphosphate carboxylase small chain precursor
153	12.7/6.4	20.6/8.3	333/279	IIGFDNVR AHGSLPGYYDGR FETLSYLPPLSR EQLASEIDYLLR	gi|6272551	Ribulose 1,5-bisphosphate carboxylase small chain precursor
154	12.3/6.6	20.6/8.3	336/267	VPGYYDGR IIGFDNVR AHGSLPGYYDGR FETLSYLPPLSR EQLASEIDYLLR	gi|6272551	Ribulose 1,5-bisphosphate carboxylase small chain precursor
21	72.1/7.3	55.5/5.9	74/59	VENQEGVINFDEILR	gi|15242313	Pyruvate kinase
31	64.5/6.2	17.7/5.9	106/64	EEVFGPVAPLLR IANDTNAGLAAYIFTNNIQR	gi|15219379	Aldehyde dehydrogenase
32	63.3/6.3	17.7/5.9	178/116	EEVFGPVAPLLR IANDTNAGLAAYIFTNNIQ	gi|15219379	Aldehyde dehydrogenase
33	63.3/6.5	17.7/5.9	119/84	EEVFGPVAPLLR IANDTNAGLAAYIFTNNIQ	gi|15219379	Aldehyde dehydrogenase
51	53.4/5.6	42.1/5.4	266/180	YSLKPLVPR YLKPSVAGFLMQK YLKPSVAGFLMQK LAALADVYVNDAFGTAHR	gi|21536853	Phosphoglycerate kinase
53	53.4/5.8	42.1/5.4	228/182	YSLKPLVPR LAALADVYVNDAFGTAHR VDLNVPLDDNSNITDDTR	gi|21536853	Phosphoglycerate kinase
52	51.9/5.6	42.5/5.9	88/60	VDLNVPLDDNFNITDDTR	gi|29124969	Phosphoglycerate kinase
57	52.9/6.6	36.7/8.3	130/99	LVSWYDNEWGYSTR GILGYTEDDVVSTDFVGDSR	gi|120666	Glyceraldehyde-3-phosphate dehydrogenase
60	51.0/6.9	36.7/8.3	283/210	LVSWYDNEWGYSTR FGIVEGLMTTVHSITATQK GILGYTEDDVVSTDFVGDSR	gi|120666	Glyceraldehyde-3-phosphate dehydrogenase
58	51.0/6.5	36.7/7.0	384/307	VPTVDVSVVDLTVR LVSWYDNEWGYSTR FGIVEGLMTTVHSITATQK GILGYTEDDVVSTDFVGDSR	gi|51703306	Glyceraldehyde 3-phosphate dehydrogenase
59	50.0/6.7	36.2/6.6	85/45	TFAEEVNAAFR GILSVCDEPLVSIDFR	gi|17942960	Glyceraldehyde 3-phosphate dehydrogenase
61	50.5/7.0	32.2/6.8	250/185	VPTVDVSVVDLTVR LVSWYDNEWGYSTR GILGYTEDDVVSTDFIGDNR	gi|62816190	Glyceraldehyde-3-phosphate-dehydrogenase
62	52.9/7.0	22.4/8.4	143/89	VPTVDVSVVDLTVR GILGYTEEDVVSTDFIGDSR	gi|75859953	Glyceraldehyde-3-phosphate dehydrogenase
64	51.9/7.2	36.5/6.6	87/40	TFAEEVNAAFR	gi|66026	Glyceraldehyde-3-phosphate dehydrogenase
65	51.5/7.5	32.2/7.0	–/52	YDTVHGKWK	gi|82400215	Glyceraldehyde 3-phosphate dehydrogenase
66	51.3/8.0	32.2/7.0	156/136	YDTVHGQWK TLLFGEKPVTVFGVR	gi|15221116	Lactoylglutathione lyase
68	47.3/5.0	34.3/5.6	83/33	LIVVVFPSFGER	gi|92874757	Pyridoxal-5-phosphate-dependent enzyme, beta subunit (cysteine synthase)
69	48.6/5.2	20.8/5.4	83/65	FFDPDFYR ILHAPIEPYNTGFLK	gi|30679088	Aminopeptidase
86	39.9/4.6	35.1/5.9	177/131	GGSTGYDNAVALPAGGR DGIDYAAVTVQLPGGER LTYTLDEIEGPFEVSPDGTVK	gi|19157	33 kDa precursor OEC protein
87	39.6/4.7	35.1/5.9	354/304	GGSTGYDNAVALPAGGR DGIDYAAVTVQLPGGER LTYTLDEIEGPFEVSPDGTVK	gi|19157	33 kDa precursor OEC protein
113	28.8/5.8	28.6/8.5	53/42	EFPGQVLR	gi|21265	23 kDa OEC protein
140	18.0/6.2	13.9/5.8	69/54	TNAENEFVTIK	gi|109892873	33 kDa subunit of oxygen evolving system of photosystem II
143	15.5/9.6	13.9/5.8	77/62	TNAENEFVTIK	gi|109892873	33 kDa subunit of oxygen evolving system of photosystem II
89	42.3/4.8	53.9/7.0	68/57	AGFAGIILEDQVSPK	gi|50926276	OSJNBa0014K14.16, PEP phosphonomutase
90	41.9/4.9	37.6/5.0	162/119	LFNAVAAEDLIVK IVVSSCGHDGPFGATGVK	gi|58201024	Thiamine biosynthetic enzyme
99	36.4/5.9	28.4/1.0	73/–		gi|37721410	Photosystem II subunit H
100	34.1/5.8	57.4/6.8	67/40	IIDLLTGLQGR	gi|15231538	CYP71B34 (Cytochrome P450)
144	14.5/9.6	16.2/6.3	112/98	GLVGEIIGR GDYAIDIGR	gi|62114996	Nucleoside diphosphate kinase
145	14.5/9.6	19.3/6.3	180/155	GDYAIDIGR NVIHGSDSVESAR IIGATNPGDSAPGTIR	gi|1346675	Nucleoside diphosphate kinase B
Cell growth/division						
44	63.8/4.6	50.5/4.7	256/72	LAVNLIPFPR FPGQLNSDLR GHYTEGAELIDSVLDVVR	gi|4415990	Beta-tubulin 1
45	61.5/4.7	59.1/4.9	425/313	QLFHPEQLISGK LVSQVISSLTASLR SLDIERPTYTNLNR AVFVDLEPTVIDEVR FDGALNVDVTEFQTNLVPYPR	gi|20413	Alpha-tubulin
46	61.5/4.8	59.1/4.9	229/117	QLFHPEQLISGK LVSQVISSLTASLR AVFVDLEPTVIDEVR	gi|20413	Alpha-tubulin
Transcription and protein synthesis						
39	57.6/6.6	77.4/7.1	–/39	EFRAMVEER	gi|13111324	110 kDa 4SNc-Tudor domain protein
98	33.1/5.6	21.0/1.0	75/–		gi|18027946	Ribosomal protein S4
131	23.2/9.9	19.8/9.9	147/111	AMQLLESGLK VLEQLSGQTPVFSK	gi|49333381	Putative ribosomal protein

Table 1 (*Continued*)

Spot n.[a]	MW (kDa)/p*I*		Prot. score/ion score[c]	Seq. ID Peptides[d]	ID (NCBI)[e]	Protein description
	Exp.[b]	Theor.[b]				
134	17.6/10	16.3/10.7	101/72	TPGPGAQSALR IEDVTPIPTDSTR	gi|83284009	Ribosomal protein S14-like protein
121	20.5/5.4	17.8/5.7	63/46	TFPQQAGTIR LPTDENLLSQIK	gi|14193249	Translation initiation factor 5A
142	16.1/7.4	16.8/5.4	75/58	GFGFVTFSNEK	gi|2267569	Glycine-rich RNA binding protein 2
Protein destination and storage						
3	75.6/4.4	75.4/5.1	296/233	DIDEVILVGGSTR QFAAEEISAQVLR AVVTVPAYFNDSQR	gi|1143427	Heat shock protein 70
5	80.7/4.6	80.3/4.9	324/205	APFDLFDTR EDQLEYLEER GIVDSEDLPLNISR HNDDEQYVWESQAGGSFTVTR	gi|38154482	Molecular chaperone Hsp90-1
6	84.6/4.6	16.5/3.8	93/65	VFISDDFDGELFPR	gi|68565555	Putative heat shock protein HSP90
93	36.7/6.6	23.3/8.7	67/51	LTVEDPVTVEYITR	gi|14594917	Putative alpha4 proteasome subunit
94	33.4/4.2	26.1/4.7	157/107	ITSPLLEPSSVEK DLTLQEAETIALSILK	gi|7839485	20S proteasome subunit
124	21.5/6.2	26.7/9.3	80/52	DFMIQGGDFDK	gi|50931055	Cyclophilin
125	19.4/6.2	18.3/8.3	220/202	FADENFVK HVVFGQVVEGLDVVK	gi|829119	Cyclophilin
126	19.0/8.5	13.3/8.8	133/112	HVVFGQVVEGLDVVK	gi|38566732	Cyclophilin-type
127	19.6/8.7	18.3/8.9	144/110	FADENFIK VFFDMTVGGAPAGR	gi|18076088	Cyclophilin
163	8.6/6.7	15.0/6.7	104/30	EGIPPDQQR	gi|33327286	Polyubiquitin 2
Transporters						
79	43.5/8.4	29.4/7.7	91/73	SLFTISGEVDTR ASALIQHEWRPK	gi|515360	36 kDA porin II
81	38.1/8.3	29.5/9.1	90/90	KGELFLGDVNTQLK	gi|396819	Porin
101	33.7/6.1	23.3/6.7	106/72	HLTGEFEK NLQYYEISAK	gi|495731	Small ras-related protein
Cell structure						
48	56.5/4.8	41.9/5.3	137/54	IWHHTFYNELR NYELPDGQVITIGAER	gi|32186916	Actin
49	56.5/4.9	41.9/5.3	524/364	GYMFTTTAER GEYDESGPSIVHR IWHHTFYNELR NYELPDGQVITIGAER VAPEEHPVLLTEAPLNPK DLYGNIVLSGGSTMFPGIADR	gi|32186892	Actin
Signal transduction						
75	44.3/6.6	36.0/5.3	108/102	SLEEDVAYHTTGDFR	gi|4580920	Vacuole-associated annexin VCaB42
76	45.1/7.1	16.7/9.6	106/62	LWDLATGVSAR AHTDQVTAIATPIDNPDMIVTSSR	gi|3023858	Guanine nucleotide-binding protein subunit beta-like protein
83	39.6/4.3	29.9/4.7	221/165	DSTLIMQLLR TVDVEELTVEER SAQDIALADLAPTHPIR	gi|67107029	14-3-3 protein
84	39.6/4.4	29.4/4.7	147/90	TVDVEELTVEER SAQDIALAELAPTHPIR	gi|44917153	14-3-3 e -2 protein
148	14.1/3.6	16.8/4.1	107/82	DQDGFISAAELR EADVDGDGQINYEEFVK	gi|354318	Calmodulin
Disease/defense						
18	65.1/7.0	57.3/6.5	165/94	TWPEDILPLQPVGR EGNFDLVGNNFPVFFIR	gi|12002676	Catalase
34	64.5/6.7	57.6/6.8	283/170	TFAYADTQR SHIQEYWR FPDVIHAFKPNPK EGNFDIVGNNFPVFFIR	gi|5759096	Catalase CAT1
36	63.8/6.9	57.6/6.8	354/191	TFAYADTQR SHIQEYWR DEEVDYFPSR IWPEDIFPLQQIGR EGNFDIVGNNFPVFFIR	gi|5759096	Catalase CAT1
24	56.0/8.3	26.6/8.3	70/43	DIGQAAGVLR DSVVLTGGPDYDVPLGR	gi|14029184	Peroxidase
91	37.4/5.1	27.7/5.3	132/54	YAADEEAFFADYAESHM	gi|62526589	Ascorbate peroxidase APX3
108	31.6/7.0	29.5/9.0	72/65	GGFPLPTLTHR	gi|1220537	Osmotin-like protein (Thaumatin)
109	32.2/7.2	20.7/5.2	–/40	MASSVGFLDSHIPSQK	gi|15222591	Serine-type endopeptidase inhibitor
114	31.6/5.9	22.9/5.8	134/82	HHQTYITNYNK	gi|5777414	Superoxide dismutase, MnSOD
122	20.1/5.6	17.5/5.5	64/54	FALLVDDLK	gi|19548660	Peroxiredoxin
139	17.8/5.2	17.1/5.7	75/47	EYPNSYVFIIDMPGLK	gi|1350517	Heat shock protein 17.0
Secondary metabolism						
72	46.4/5.6	25.4/8.6	127/103	FGHPTFALVR FVPSEFGNDVDR	gi|76559894	Isoflavone reductase-like protein 5
Others						
40	57.6/6.8	111.7/5.8	48/48	KEMSIAFEAER EMSIAFEAER	gi|15219527	Unknown protein
41	57.6/6.9	111.7/5.8	–/55	KEMSIAFEAER EMSIAFEAER	gi|15219527	Unknown protein
120	20.5/5.2	79.5/8.7	59/36	NSMVDEAFR	gi|3258568	Unknown protein
67	46.0/4.8	32.7/5.4	131/94	DPDGYIFELIQR	gi|2213425	Hypothetical protein
136	17.0/4.6	49.1/4.4	72/–		gi|108864159	Expressed protein
141	17.3/6.4	49.1/4.4	72/–		gi|108864159	Expressed protein
159	11.6/5.7	49.1/4.4	70/–		gi|108864159	Expressed protein
162	9.6/6.6	49.1/4.4	67/–		gi|108864159	Expressed protein
147	15.8/4.0	27.0/7.7	63/36	GTNAEQALAR	gi|91806037	Seven in absentia protein

[a] Number of each spot from 2-DE.
[b] Molecular mass and p*I* experimental and theoretical.
[c] Protein score and ion score.
[d] Sequence of identified peptides from MS/MS searches.
[e] Identification of first protein hit using non-redundant NCBI database.

mass spectrometry. Representative MS/MS data, an experimentally determined peptide sequence, and a database search results are shown in Fig. 3. For protein identification, the normal MASCOT criterion was used (i.e., score > 37). Using this criterion, proteins from 86 of the 163 spots were identified (Table 1), yielding a protein identification success rate of 53%, even though no EST database for embryogenic tissues of cassava is available. This value is comparable with the previously reported protein identification success rates of 55% for embryogenic cell suspension cultures of *Medicago truncatula* [22] and cowpea [15] and 62% for early somatic embryogenesis in *Pica glauca* [11]. The procedures we present here for protein extraction and identification can be

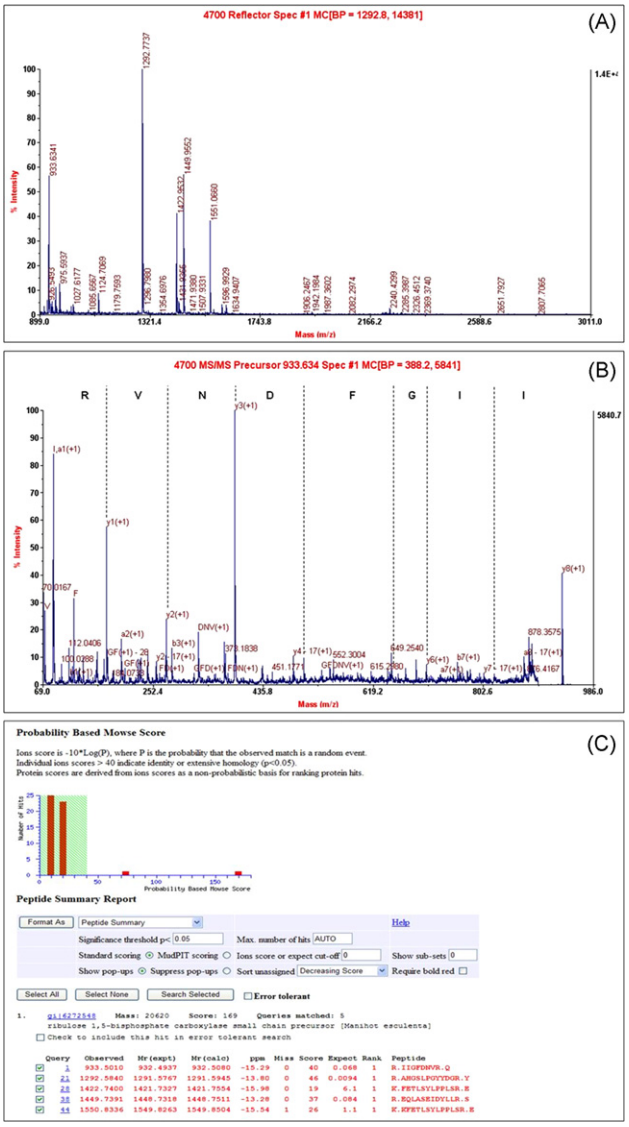

Fig. 3. Representative MS/MS data obtained on an ABI 4700 Proteomics Analyzer for spot 153: (A) mass spectra of peptides generated by the digestion of spot 153 with trypsin; (B) tandem MS/MS mass spectra and experimentally determined sequence for peptide sequence observed at *m*/*z* 933.634; (C) database search result.

applied to a few milligrams of tissue and following protein extraction and the precipitation/washing steps, the powdered sample can be readily dissolved in the solution used for the rehydration of the IPG strips and electrofocused. The protein patterns in the 2D-gels are reproducible and no signs of protein modification/degradation can be observed. The obtention of a protein identification success rate of 53% demonstrate that the procedure for protein extraction and 2D electrophoresis are compatible with mass spectrometry analysis. These procedures will provide a novel opportunity for preparing 2-DE reference maps and protein identification of cassava tissues.

The identified proteins were classified according to their main function, as suggested by Imin et al. [22]: protein involved in metabolism and energy (43% of identified proteins), protein destination and storage (11.6%), disease/defense (11.6), transcription and protein synthesis (7%), signal transduction (5.8%), cell growth/division (3.5%), transporters (3.5%), cell structure (2.3%), secondary metabolism (1.2%) and other functional classes (10.5%). The relative abundance of metabolic enzymes has also been observed in embryogenic cell suspensions, roots and seeds of *M. truncatula* [14,22,23], in fungal elicitor-treated *Arabidopsis* cell cultures [24] and in embryogenic cell suspensions of cowpea [15]. The abundance of proteins related to energy metabolism in developing secondary somatic embryos of cassava, may be explained by the high metabolic activity necessary to sustain the intense cell division activity in the developing embryos (Fig. 1).

The relative proportion of the protein classes identified in the present work, was similar to that of the cassava root proteome [10], but several of the proteins identified in the SSE proteome were not identified in the cassava root proteome, as was the case, for example, for β-tubulin and annexin—proteins that are associated with cell cycle events [25]. Tubulins are associated with cell division and cell enlargement aspects of the cell cycle. During cell division, they play an important role in separation of the organelles and daughter chromosomes (mitosis). As for the annexins, there is strong evidence that they directly involved in cell division [25]. For example, they accumulate during the cell cycle and peak at the end of mitosis in tobacco (*Nicotiana tabacum*) cells [26]. Because they are localized at cell junctions and are known to bind secretory vesicles during exocytosis, annexins could play a role in cell wall maturation during cell division [26]. However, as the methods of protein extraction for establishing the proteomes of SSE and of roots were based in different solubility criteria, this can account for the differences observed between the SSE and root proteomes. Additionally, the limited number of proteins (86 and 292, respectively) identified in both proteomes does not allow for ascertaining the putative role of these proteins either in SSE or in root development.

4. Conclusions

Despite the importance of somatic embryogenesis as a tool for cassava biotechnology, very little is known about the mechanisms underlying the induction, development and germination of somatic embryos. In this study we present a histological analysis of the induction of SSE from green cotyledons of somatic embryos and the first data profiling the proteome of SSE. The use of histological techniques has shown that in cassava, somatic embryos emerge from competent embryogenic cells as a result of intense mitotic activity induced in the procambium region by the incubation of pieces of green cotyledons of somatic embryos with the auxin picloram. As incubation proceeds, embryogenic masses are formed around the procambium throughout the explant and later these masses fuse together, subsequently giving rise to the somatic embryos, thus indicating that somatic embryos of cassava have a multicellular origin. The use of proteomics as a tool for global expression analysis has been shown to be efficient and effective in protein identification in cassava SSE. Approximately 410 proteins spots were resolved by 2-DE and subsequent analysis led to the identification of 86 proteins. These proteins may serve as molecular markers for the developmental stages of cassava somatic embryos, as well as to discriminate between embryogenic and non-embryogenic genotypes and targets for further biochemical and physiological characterizations. The pending release of the complete cassava genome by the Cassava Genome Sequencing Initiative will greatly aid in identifying, not only the remaining proteins observed in the 2-DE gels here shown, but also in unraveling the proteome of the whole process of induction and development of somatic embryos in cassava that we will focus on in the future.

References

[1] M. Stupak, H. Vanderschuren, W. Gruissem, P. Zhang, Biotechnological approaches to cassava protein improvement, Trends Food Sci. Technol. 17 (2006) 634–641.
[2] N. Taylor, P. Chavarriaga, K. Raemakers, D. Siritunga, P. Zhang, Development and application of transgenic technologies in cassava, Plant Mol. Biol. 56 (2004) 671–688.

[3] N.J. Taylor, M. Edwards, R.J. Kiernan, C.M.D. Davey, D. Blakestey, G.G. Henshaw, Development of friable embryogenic callus and embryogenic suspension systems in cassava (*Manihot esculenta* Crantz), Nat. Biotechnol. 14 (1996) 726–730.
[4] P. Zhang, G. Legris, P. Coulin, J. Puonti-Kaerlas, Production of stably transformed cassava plants via particle bombardment, Plant Cell Rep. 19 (2000) 939–945.
[5] B.B. Hankoua, N.J. Taylor, S.Y.C. Ng, I. Fawole, J. Puonti-Kaerlas, C. Padmannabhan, J.S. Yadav, C.M. Fauquet, A.G.O. Dixon, Production of the first transgenic cassava in Africa via direct shoot organogenesis from friable embryogenic calli and germination of maturing somatic embryos, Afr. J. Biotechnol. 5 (2006) 1700–1712.
[6] U. Ihemere, D. Arias-Garzon, S. Laerence, R. Sayre, Genetic modification of cassava for enhanced starch production, Plant Biotech. J. 4 (2006) 453–465.
[7] T. Feitosa, J.L.P. Bastos, L.F.A. Ponte, T.L. Jucá, F.A.P. Campos, Somatic embryogenesis in cassava genotypes from the northeast of Brazil, Braz. Arch. Biol. Technol. 50 (2007) 201–206.
[8] J. Groll, D.J. Mycock, V.M. Gray, S. Laminski, Secondary somatic embryogenesis of cassava on picloram supplemented medium, Plant Cell Tiss. Org. Cult. 65 (2001) 201–210.
[9] C. Lopez, V. Jorge, B. Piegu, C. Mba, D. Cortes, S. Restrepo, M. Soto, M. Laudie, C. Berger, R. Cooke, M. Delseny, J. Tohme, V. Verdier, A unigene catalogue of 5700 expressed genes in cassava, Plant Mol. Biol. 56 (2004) 541–554.
[10] J. Sheffield, N. Taylor, C. Fauquet, S. Chen, The cassava (*Manihot esculenta* Crantz) root proteome: protein identification and differential expression, Proteomics 6 (2006) 1588–1598.
[11] D. Lippert, J. Zhuang, S. Ralph, D.E. Ellis, M. Gilbert, R. Olafson, K. Ritland, B. Ellis, C.J. Douglas, J. Bohlmann, Proteome analysis of early somatic embryogenesis in *Picea glauca*, Proteomics 5 (2005) 461–473.
[12] N. Imin, M. Nizamidin, D. Daniher, K.E. Nolan, R.J. Rose, B.G. Rolfe, Proteomic analysis of somatic embryogenesis in *Medicago truncatula*. Explant cultures grown under 6-benzylaminopurine and 1-naphthaleneacetic acid treatments, Plant Physiol. 137 (2005) 1250–1260.
[13] T. Winkelmann, D. Heintz, A. Van Dorsselaer, M. Serek, H.-P. Braun, Proteomic analyses of somatic and zygotic embryos of *Cyclamen persicum* Mill. Reveal new insights into seed and germination physiology, Planta 224 (2006) 508–519.
[14] F.D. Jong, U. Mathesius, N. Imin, B.G. Rolfe, A proteome study of the proliferation of cultured *Medicago truncatula* protoplasts, Proteomics 7 (2007) 722–736.
[15] F.C.S. Nogueira, E.F. Gonçalves, E.S. Jereissati, M. Santos, J.H. Costa, O.B. Oliveira-Neto, A.A. Soares, G.B. Domont, F.A.P. Campos, Proteome analysis of embryogenic cell suspensions of cowpea (*Vigna unguiculata*), Plant Cell Rep. 26 (2007) 1333–1343.
[16] M. Marsoni, M. Bracale, L. Espen, B. Prinsi, A. Negri, C. Vannini, Proteomic analysis of somatic embryogenesis in *Vitis vinifera*, Plant Cell Rep. 27 (2008) 347–356.
[17] E.A.R. Vasconcelos, F.C.S. Nogueira, E.F.M. Abreu, E.F. Gonçalves, P.A.S. Souza, F.A.P. Campos, Protein extraction from cowpea tissues for 2D electrophoresis and MS analysis, Chromatographia 62 (2005) 447–450.
[18] T. Murashige, F. Skoog, A revised medium for rapid growth and bioassays with tobacco tissue culture, Physiol. Plant 15 (1962) 473–497.
[19] J.A. Fernando, M.L.C. Vieira, I.O. Geraldi, B. Appezzato-da-Gloria, Anatomical study of somatic embryogenesis in *Glycine max* (L.) Merril., Braz. Arch. Biol. Technol. 45 (2002) 277–286.
[20] M.C. Dornellas, M.L. Vieira, B. Appezzato-da-Gloria, Histological analysis of organogenesis and somatic embryogenesis induced in immature tissues of *Stylosanthes scabra*, Ann. Bot. 70 (1992) 477–482.
[21] A.P.M. Rodriguez, H.Y. Wetzstein, The effect of auxin type and concentration on pecan (*Carya illinoiensis*) somatic embryo morphology and subsequent conversion into plants, Plant Cell Rep. 13 (1994) 607–611.
[22] N. Imin, F.D. Jong, U. Mathesius, G. Noorden, N.A. Saeed, X.-D. Wang, R.J. Rose, B.G. Rolfe, Proteome reference maps of *Medicago truncatula* embryogenic cell cultures generated from single protoplasts, Proteomics 4 (2004) 1883–1896.
[23] Z. Lei, A.M. Elmer, B.S. Watson, R.A. Dixon, P.J. Mendes, L.W. Sumner, A two-dimensional electrophoresis proteomic reference map and systematic identification of 1367 proteins from a cell suspension culture of the model legume *Medicago truncatula*, Mol. Cell Prot. 4 (2005) 1812–1825.
[24] S. Chivasa, J.M. Hamilton, R.S. Pringle, B.K. Ndimba, W.J. Simon, K. Lindsey, A.R. Siabas, Proteomic analysis of differentially expressed proteins in fungal elicitor-treated *Arabidopsis* cell cultures, J. Exp. Bot. 57 (2006) 1553–1562.
[25] K. Gallardo, C. Signor, J. Vandekerckhove, R.D. Thompson, J. Burstin, Proteomics of *Medicago truncatula* seed development establishes the time frame of diverse metabolic processes related to reserve accumulation, Plant Phys. 133 (2003) 664–682.
[26] J. Proust, G. Houlne, M.L. Schantz, W.H. Shen, R. Schantz, Regulation of biosynthesis and cellular localization of Sp32 annexins in tobacco BY2 cells, Plant Mol. Biol. 39 (1999) 361–372.